

Dynamics of Biofuel Stock Prices: A Bayesian Approach

Xiaodong Du, Dermot J. Hayes, and Cindy Yu

Working Paper 09-WP 498
September 2009

**Center for Agricultural and Rural Development
Iowa State University
Ames, Iowa 50011-1070
www.card.iastate.edu**

Xiaodong Du is a postdoctoral research associate in the Center for Agricultural and Rural Development, Dermot Hayes is a professor in the Department of Economics and Department of Finance and in the Center for Agricultural and Rural Development, and Cindy Yu is an assistant professor in the Department of Statistics, all at Iowa State University.

This paper is available online on the CARD Web site: www.card.iastate.edu. Permission is granted to excerpt or quote this information with appropriate attribution to the authors.

Questions or comments about the contents of this paper should be directed to Xiaodong Du, 565 Heady Hall, Iowa State University, Ames, Iowa 50011-1070; Ph: (515) 294-8015; Fax: (515) 294-6336; E-mail: xdu@iastate.edu.

| |
|---|
| Iowa State University does not discriminate on the basis of race, color, age, religion, national origin, sexual orientation, gender identity, sex, marital status, disability, or status as a U.S. veteran. Inquiries can be directed to the Director of Equal Opportunity and Diversity, 3680 Beardshear Hall, (515) 294-7612. |
|---|

Abstract

We use Bayesian Markov Chain Monte Carlo methods to investigate the linkage between the volatility of ethanol security prices and the uncertainty surrounding the profitability of ethanol production and the price variations of non-ethanol energy securities. The joint evolution of return and volatility is modeled as a stochastic process that incorporates jumps in both return and volatility. While a strong and significant correlation is found between the volatility of ethanol securities and profit uncertainty from June 2005 to July 2008, the dynamic pattern of ethanol stock volatility is strikingly similar to that of the S&P 500 energy sector index in the more recent period. Our evidence lends support to the findings in the literature on rational learning from uncertainty in determining the equity price and volatility during the adoption and development of a technological innovation.

Keywords: jumps, rational learning, stochastic volatility, technological innovation.

JEL classification: C11; G12; Q42.

1. Introduction

Production of corn-based ethanol in the United States increased from 3.9 million gallons in 2005 to 9.0 million gallons in 2009 (RFA 2009). The Renewable Fuel Standard (RFS), a provision of the Energy Policy Act of 2005, mandated 5.4 billion gallons of renewable fuels be blended into gasoline in 2008 and 7.5 billion gallons by 2012. The Energy Independence and Security Act of 2007 further expanded the short-term targets for corn-based ethanol production and consumption (9 billion gallons by 2008) and the long-term targets (15 billion gallons by 2022). A high oil price, an import tariff that protects domestically produced ethanol from imports, and tax credits for refiners who blend ethanol have stimulated investments in the biofuels industry and related publicly traded securities.

There was a boom of ethanol IPOs (initial public offerings, the first step to becoming a publicly traded company) over the period 2004-2006. The amount of money raised through the flow of clean technology company IPOs was over \$50 billion, even without accounting for the institutional and private investments (WSJ 2008). A number of ethanol producers later became publicly traded companies on the stock markets. By the end of 2007, the renewable energy sector had a market cap of about \$170 billion, while the majority of companies had market valuations below \$500 million and a few of them never generated any revenues from production. In addition, biofuel stock prices have shown a common volatile and bubble-like pattern. After an initial surge in May 2006, stock prices fell in the presence of high volatility in crude oil and corn prices. The rapid expansion in biofuel investments may have exhibited wasteful overinvestment. This is indicated by the fact that numerous established producers have filed for Chapter 11 bankruptcy protection. While these phenomena could be attributed to market irrationality, they might also reflect market uncertainty about ethanol's future profitability. The time-

varying nature of this uncertainty could produce excess volatility and observed price behavior. In this study, we attempt to determine if the patterns we observe could be attributed to market irrationality, or whether that they can be explained by the market's rational learning from uncertainty associated with contingent profitability of ethanol production.

The dynamic properties of stock prices and price variations have been extensively investigated in the literature; however, the studies on the evolution of biofuel stock prices are sparse. One exception is Henriques and Sadorsky (2008). The authors examine the interactions among alternative energy stock prices, technology stock prices, oil prices, and interest rates. Technological stock prices and oil prices are shown to Granger-cause changes in alternative energy stock prices, while shocks to technology stock prices have a larger impact.

A few studies link stock price changes to technological revolution and firms' intangible capital accumulation to explain stock market run-ups in the 1920s and 1990s (e.g., Hall 2001; Hobijn and Jovanovic 2001; Laitner and Stolyarov 2003; Nicholas 2008). The most relevant is Pastor and Veronesi (2009). In a general equilibrium model, they investigate the bubble-like stock prices of firms that employ a new technology during technology revolutions. The generated stock price pattern is proved to be consistent with the characteristics of technology revolutions, including high uncertainty and fast adoption, and investors' rational expectations. The basic argument is that, as a new technology emerges, investors are highly uncertain about its future productivity because of the small scale of initial production and a low probability of large-scale adoption. The nature of the risk associated with this uncertainty varies over time, which may produce observed stock price patterns and also have important implications for price volatility.

In a related study seeking to understand the role of learning in financial markets, Pastor and Veronesi (2003, 2006) argue that the observed high valuation of NASDAQ stocks during the Internet booms in the late 1990s was mainly driven by high uncertainty of the dividend growth rate of the innovative firms. The initial overinvestment associated with technological revolutions could also be rationalized as an efficient way of learning about returns to scale in a new industry, as shown by Johnson (2007) and DeMarzo, Kaniel and Kremer (2007).

In the current study, we first examine the dynamic behavior of biofuel stock prices during the recent expansion by comparing the level and volatility of biofuel stock prices with those of traditional energy stocks. A biofuel stock price index is constructed as a proxy for the stock prices of major publicly traded ethanol producers, while the S&P 500 energy sector index (SPNY) represents stock prices of various companies in the traditional energy sector. We limit our consideration to companies producing corn-based ethanol. This is the most mature biofuel production technology in the United States.

The daily returns and volatilities of price indices for biofuels and energy stocks are modeled in a stochastic volatility model with correlated Merton jumps in returns and volatility. The estimation is done using the Bayesian Markov Chain Monte Carlo (MCMC) technique. A data augmentation approach is employed to obtain the latent volatility variables. We further analyze the relationship between the estimated volatility and profit uncertainty associated with ethanol production.

In the next section, we establish the empirical model and briefly describe the Bayesian MCMC simulator used to characterize the posterior distribution of the parameters of interest. Details of the Gibbs sampler algorithm and simulation study are deferred to the Appendices. Section 3 describes the data construction procedure and

resources of collection. Our empirical results are presented in Section 4, and Section 5 concludes with a summary.

2. Empirical Model and Bayesian Simulator

2.1 The Model

To fully capture the dynamics of biofuel stock prices, we apply the stochastic volatility model with correlated Merton jumps in returns and volatility (SVC MJ). The model was first proposed by Eraker, Johannes and Polson (2003, hereafter EJP) belonging to the class of affine jump-diffusion models in Duffie, Pan and Singleton (2000). Assuming that asset prices are driven by a continuous diffusion process and discontinuous Poisson jumps, the SVC MJ model provides a parsimonious and tractable method to estimate the time-varying volatility of returns. The model is motivated by recent studies documenting the need to simultaneously incorporate jumps in returns and volatility in order to better represent the observed price dynamics (e.g., Anderson, Benzoni and Lund 2002; Chernov et al. 2003). Specifically, while jumps in returns generate infrequently observed sudden changes in asset prices, incorporating jumps in volatility captures the rapid increases in volatility process and may remove model misspecification and significantly improve model performance (EJP 2003).

We assume that the logarithm of stock price, $Y_t = \log(S_t)$, satisfies the following stochastic differential equations:

$$(1) \quad \begin{pmatrix} dY_t \\ dV_t \end{pmatrix} = \begin{pmatrix} \mu \\ \kappa(\theta - V_{t-}) \end{pmatrix} dt + \sqrt{V_{t-}} \begin{pmatrix} 1 & 0 \\ \rho\sigma_v & \sqrt{1-\rho^2}\sigma_v \end{pmatrix} dW_t + \begin{pmatrix} dJ_t^y \\ dJ_t^v \end{pmatrix}$$

where $V_{t-} = \lim_{s \uparrow t} V_s$, V_t is the instantaneous volatility, W_t is a standard Brownian motion in \mathbb{R}^2 , and jumps in returns and volatility are represented by J_t^y and J_t^v , respectively.

While μ measures the mean return, κ is the speed of mean reversion of volatility, θ is the long-run mean of stochastic volatility, and σ_v is the so-called volatility of volatility measure. The correlation between returns and instantaneous volatility is denoted by ρ . Without jumps in returns and volatility, model (1) reduces to the square-root stochastic volatility model in Heston (1993). Model (1) is the same as the stochastic volatility with jumps in returns model presented in Bates (1996) while jumps in volatility are not included.

To model daily stock prices, we apply the first-order Euler discretized version of the continuous time model specified in (1) with the discretization interval $\Delta = 1 / 250$.¹ The discretized empirical model is

$$(2) \quad \begin{aligned} Y_{(t+1)\Delta} &= Y_{t\Delta} + \mu\Delta + \sqrt{V_{t\Delta}}\Delta\varepsilon_{(t+1)\Delta}^y + J_{(t+1)\Delta}^y \\ V_{(t+1)\Delta} &= V_{t\Delta} + \kappa(\theta - V_{t\Delta})\Delta + \sigma_v\sqrt{V_{t\Delta}}\Delta\varepsilon_{(t+1)\Delta}^v + J_{(t+1)\Delta}^v \end{aligned}$$

where $\varepsilon_{(t+1)\Delta}^y$ and $\varepsilon_{(t+1)\Delta}^v$ are $N(0,1)$ random errors with correlation ρ . The correlated error specification attempts to capture the leverage effect, a negative correlation between current returns and future volatility (Nelson 1991). The jumps in returns and volatility are defined as $J_{(t+1)\Delta}^y = \xi_{(t+1)\Delta}^y N_{(t+1)\Delta}$ and $J_{(t+1)\Delta}^v = \xi_{(t+1)\Delta}^v N_{(t+1)\Delta}$, respectively, where the contemporaneous jump arrivals $N_{(t+1)\Delta}$ follow a Poisson processes with constant intensity λ , i.e., $P(N_{(t+1)\Delta} = 1) = \lambda\Delta$ for small delta. The jump sizes, ξ_{t+1}^y and ξ_{t+1}^v , are correlated with coefficient ρ_J , and distributed as $\xi_{(t+1)\Delta}^v \sim \exp(\mu_v)$, and $\xi_{(t+1)\Delta}^y | \xi_{(t+1)\Delta}^v \sim N(\mu_y + \rho_J \xi_{(t+1)\Delta}^v, \sigma_y^2)$.

The SVCMJ model has the significant advantage of containing three factors simultaneously (EJP 2003). These are the diffusive stochastic volatility, the jump in

¹ Using daily price data, EJP (2003) prove that the discretization method does not show a significant bias.

returns, and jump in volatility, each of which has a different impact on the distribution of returns. While diffusive stochastic volatility and jumps in returns generate unconditional and conditional non-normality in returns consistent with empirical findings, jumps in volatility capture a rapidly changing but persistent component in volatility dynamics.

2.2 Bayesian Estimation

This section describes the Bayesian MCMC estimation method for the discretized SVCMJ model specified in (2). Estimation of double jump processes is challenging because the high dimensionality of latent variables, such as stochastic volatility, jump sizes and times in both returns and volatility significantly complicates the estimation. Computationally it is almost impossible to integrate the large number of latent variables when implementing either likelihood or moment-based approaches. To overcome this difficulty, we adopt a Bayesian MCMC method for the estimation. Compared with other estimation methods of stochastic volatility models such as efficient method of moments (EMM), simulated maximum likelihood (e.g., Brandt and Santa-Clara 2002), and generalized method of moments (GMM) (e.g., Pan 2002), a Bayesian approach is particularly suitable, having been proven to perform well and produce relatively accurate results.

In model (2) only stock returns $(Y_t)_{t=1}^{T+1}$ are observable; stochastic volatility $(V_t)_{t=1}^{T+1}$, jump times $(N_t)_{t=1}^T$, and jump sizes $(\xi_t^y)_{t=1}^T$ and $(\xi_t^v)_{t=1}^T$ are latent.² The set of parameters of interest is $\Theta = \{\mu, \kappa, \theta, \sigma_v, \rho, \lambda, \mu_v, \mu_y, \sigma_y, \rho_j\}$. The MCMC methods avoid marginalization issues by using a conditional simulation strategy. It is worth noting that

² To simplify notation, we ignore the discretization interval Δ associated with time t and $t + 1$ in the subscripts in this and in the following sections.

the Kalman Filter block updating method is difficult to model since the square-root volatility process is nonlinear, non-Gaussian and correlated with returns.

Conditioning on $V_t, N_t, \xi_t^y, \xi_t^v$, the increments for return and volatility, $Y_{t+1} - Y_t$ and $V_{t+1} - V_t$, follow a bivariate normal distribution:

$$(3) \quad \begin{bmatrix} Y_{t+1} - Y_t \\ V_{t+1} - V_t \end{bmatrix} | V_t, N_t, \xi_t^y, \xi_t^v \sim N \left[\begin{pmatrix} \mu\Delta + N_t \xi_t^y \\ \kappa(\theta - v_t)\Delta + N_t \xi_t^v \end{pmatrix}, V_t \Delta \begin{pmatrix} 1 & \rho\sigma_v \\ \rho\sigma_v & \sigma_v^2 \end{pmatrix} \right]$$

The joint distribution of $\mathbf{Y}, \mathbf{V}, \mathbf{N}, \xi^y, \xi^v$, and the parameters Θ is

(4)

$$\begin{aligned} p(\mathbf{Y}, \mathbf{V}, \mathbf{N}, \xi^y, \xi^v, \Theta) &\propto p(\mathbf{Y}, \mathbf{V} | \mathbf{N}, \xi^y, \xi^v) p(\xi^y, \xi^v | \Theta) p(\mathbf{N} | \Theta) p(\Theta) \\ &\propto \prod_{t=1}^T \frac{1}{\sigma_v V_t \Delta \sqrt{1 - \rho^2}} \exp \left\{ -\frac{1}{2(1 - \rho^2)} \left((\varepsilon_{t+1}^y)^2 - 2\rho \varepsilon_{t+1}^y \varepsilon_{t+1}^v + (\varepsilon_{t+1}^v)^2 \right) \right\} \\ &\quad \times \prod_{t=1}^T \lambda^{N_t} (1 - \lambda)^{1 - N_t} \times \prod_{t=1}^T \frac{1}{\sigma_y} \exp \left(-\frac{(\xi_t^y - \mu_y - \rho_J \xi_t^v)^2}{2\sigma_y^2} \right) \\ &\quad \times \prod_{t=1}^T \frac{1}{\mu_v} \exp \left(-\frac{\xi_t^v}{\mu_v} \right) I_{\xi_t^v > 0} \times p(\Theta) \end{aligned}$$

where $\varepsilon_{t+1}^y = \frac{Y_{t+1} - Y_t - \mu\Delta - N_t \xi_t^y}{\sqrt{V_t \Delta}}$ and $\varepsilon_{t+1}^v = \frac{V_{t+1} - V_t - \kappa(\theta - V_t)\Delta - N_t \xi_t^v}{\sigma_v \sqrt{V_t \Delta}}$, while $p(\Theta)$

denotes the joint prior distribution of model parameters.

We use convenient conjugate priors wherever possible in order to obtain standard forms of posterior distributions from which to draw directly. The following prior distributions are chosen: $\mu \sim N(0, 1)$, $\kappa \sim TN_{(0, \infty)}(0, 1)$, $\theta \sim TN_{(0, \infty)}(0, 1)$, $\mu_y \sim N(0, 100)$, $\sigma_y^2 \sim IG(5, 1/20)$, $\lambda \sim Beta(2, 40)$, $\mu_v \sim IG(10, 1/10)$, and $\rho_J \sim N(0, 4)$.³ Similar to Jacquier, Polson and Rossi (1994), (ρ, σ_v) are re-parameterized as (ϕ, ω_v) , where

³ $TN_{(a,b)}(\mu, \sigma^2)$ denotes a normal distribution with mean μ and variance σ^2 truncated to the interval (a, b) , and IG and $Beta$ represent the inverse gamma and beta distribution, respectively.

$\phi_v = \sigma_v \rho$ and $\omega_v = \sigma_v^2(1 - \rho^2)$. The priors of the transformed parameters are chosen as $\phi_v | \omega_v \sim N(0, 1/2\omega_v)$ and $\omega_v \sim IG(2, 200)$. Following Li, Wells and Yu (2008), the applied MCMC algorithm generates samples by iteratively drawing from the derived conditional posteriors, which is fully described in Appendix A.

We generate an artificial data set consisting of 1,000 data points, using the discretized model (2) with assumed true parameter values and the discretization interval $\Delta = 1/250$ to check the reliability of the Bayesian estimation approach. The 1,000 data points are chosen to be consistent with the number of observations we have for real stock price data. The estimation results on simulated data summarized in Appendix B indicate that the algorithm provides relatively accurate estimates for most of the model parameters and is capable of capturing major dynamics of the volatility path and jumps in both returns and volatility processes.

3. Ethanol Companies and Data

To investigate the biofuel stock price dynamics and link these dynamics to the uncertainty of production profitability, we construct a biofuel stock price index from the stock prices of twelve public traded companies in the U.S. ethanol sector over the period June 30, 2005 to July 9, 2009. The selected company names, trading symbols, weights used in the index, market capitalization and sample periods are listed in Table 1.

Following the construction of the S&P 500 index,⁴ the ethanol stock price index is calculated using a base-weighted-average methodology to reflect daily ethanol stock variation relative to a particular base period. Instead of using a market-capitalization-based system where weight on each stock is equal to its share in the total market values of included companies, we assign the particular weights to individual stocks based on

⁴ The calculation method for the S&P 500 index can be retrieved from <http://www.cftech.com/BrainBank/FINANCE/SandPIndexCalc.html>.

their market importance within the sector.⁵ The reason is two-fold: first, to ensure that the index does not depend on a few sector giants for its valuation; and second, to ensure that the index does not swing based on the volatility of a few thinly traded small-cap stocks.

The base period is chosen as June 30, 2005, when the ethanol stock price index starts at 30. The index is calculated as weighted daily stock prices divided by an adjustment factor where the latter is employed to maintain the consistency of the index when new stocks are brought in and some companies are removed.

The medium- and large-cap companies we consider in this study include Archer Daniels Midland (NYSE: ADM), Cosan (NYSE: CZZ), and Andersons (NASDAQ: ANDE), all of which have market capitalization of over \$300 million and are not “pure-play” ethanol companies. ADM is the second-largest corn-based ethanol producer in the United States after the privately held company POET, with an annual production capacity of more than 1 billion gallons.⁶ ADM is also the world largest processor of oilseeds, corn and wheat and operates one of the world’s largest crop origination and transportation networks. Ethanol is one of ADM’s most profitable businesses, generating about \$600 million in profit in 2007, which helped ADM’s stock price reach an all-time high of \$48.18 in April 2008.⁷ Cosan is one of the world’s largest growers and processors of sugarcane and the largest sugarcane ethanol producer in Brazil. In 2008, it manufactured over 400 million gallons of sugar-based ethanol for both domestic and international markets. The grain and ethanol group is the fastest-growing segment of Andersons’ operating ethanol manufacturing capacity of 275 million gallons in Indiana and Michigan. As a diversified agribusiness group, Andersons also owns businesses in grain processing, a retail store chain and rail transportation.

⁵ We apply the same weights used by the Biofuel Digest Index (BDI), which are determined by an expert panel (personal communication with Jim Lane, editor and publisher of *Biofuel Digest Daily*).

⁶ By the end of 2008, after a series of mergers and acquisitions, Verasun Energy became the largest ethanol producer in the U.S., but it filed for bankruptcy protection and liquidated its assets in mid-2009.

⁷ Unless otherwise stated, company information was retrieved from company Web sites.

From 2006 to 2007, while ADM and Xethanol (AMEX: XNL) were already listed on the New York Stock Exchange and the American Stock Exchange, respectively, Green Plains Renewable Energy (NASDAQ: GPRE) and BioFuel Energy (NASDAQ: BIOF) joined other publicly traded ethanol producers such as MGP Ingredients (NASDAQ: MGPI) and Pacific Ethanol (NASDAQ: PEIX) on the NASDAQ stock market. VeraSun Energy (NYSE: VSE) and Aventine Renewable Energy (OTC: AVRNQ) followed the trend to list on the New York Stock Exchange.

Green Plains Renewable Energy produces about 480 million gallons of ethanol annually, with six ethanol facilities in Indiana, Iowa, Nebraska and Tennessee. After merging with biofuels terminal company Blendstar, Green Plains also runs a number of terminal facilities throughout the southern United States. Distillery products accounted for 73% of the 2008 revenues of MGP Ingredients, with the other 27% of revenues coming from food/fuel graded alcohol and other industrial organic chemicals. Pacific Ethanol produces, markets and sells ethanol and other renewable fuels in the western United States and is the largest producer on the West Coast. Its subsidiaries that owned four ethanol plants filed for Chapter 11 bankruptcy protection on May 18, 2009. Founded in 2006, Biofuel Energy operates three large-scale ethanol production facilities located in Nebraska and Minnesota with an annual capacity of 230 million gallons of fuel-grade ethanol. VeraSun Energy was one of the leading ethanol producers in the United States, maintaining production facilities across the Midwest. Big expansions, including the acquisition of three facilities from ASAlliances Biofuels in 2007, and a merger with U.S. BioEnergy in 2008 increased VeraSun's production capacity to more than 1 billion gallons. But in October 2008, VeraSun suffered heavy losses and then filed for bankruptcy protection. By early 2009 VeraSun requested permission to liquidate its assets

and was forced to put its plants up for auction, eventually choosing Valero to buy seven facilities for \$477 million, a deal that was completed in March 2009.

We also include three relatively small ethanol companies in the biofuel price index. Global Energy Holdings Group (NYSE: GNH), formerly Xethanol Corp., operates two waste-to-ethanol facilities in Iowa. Tiger Renewable Energy (OTC: TGRW) is an international ethanol producer, focusing on China's corn ethanol market. Aventine Renewable Energy focuses on manufacturing and marketing corn-based ethanol, with two ethanol plants in Nebraska and Illinois and production of 188.8 million gallons of ethanol in 2008. It filed for bankruptcy protection on March 31, 2009.

Historical stock prices of the companies described above were collected from DataStream Advance. All prices are closing prices after adjusting for historical corporate actions including stock splits, dividends, distributions and right offerings. Daily prices of the S&P 500 energy sector index, SPNY, were also collected to represent the price trend of oil company shares.

The time series of the biofuel stock price index, which is presented in Figure 1, shows an obvious bubble-like pattern. Starting at 30 on June 30, 2005, the value of the ethanol stock index sharply increased and peaked at 78 on May 11, 2006, then gradually dropped to 50 in September 2006. After wandering in the range of 40-50 until June 2008, the index fell significantly, dropping to 20 by October 2008 and staying at that level to the end of the sample period.

Historical expected ethanol operating margins are collected from the Web site of the Center for Agricultural and Rural Development at Iowa State University.⁸ The margin is a measure of profit potential for ethanol production, which is calculated as the difference between revenues from production outputs including ethanol and distillers

⁸ The data were retrieved from http://www.card.iastate.edu/research/bio/tools/hist_eth_gm.aspx. (accessed 8 September 2009).

dried grains with solubles and various input costs such as corn and natural gas. Ethanol and corn futures prices for the nearby contracts on the Chicago Board of Trade (CBOT) and natural gas futures prices from the New York Mercantile Exchange (NYMEX) are used for the calculation of expected ethanol margins. The daily margins over the sample period are presented in Figure 2.

From late 2005 through much of 2006, high crude oil prices together with rising world energy demand drove gasoline prices to a near record high. High energy prices coupled with an increase in mandated use of ethanol in California led to higher ethanol prices. The ethanol operating margin peaked in June 2006, reaching \$3.23 per gallon. During this boom, the U.S. ethanol industry grew from 3.4 billion gallons of capacity in 2004 to 9.0 billion gallons in 2008. Excess capacity led to lower ethanol prices, and the ethanol operating margin was further reduced by high corn and natural gas prices. By July 2008, the margin was reduced to only \$0.30 per gallon and stayed at that level or even lower afterwards.

4. Estimation Results and Analysis

We define the daily uncertainty of ethanol profitability as the standard deviation of ethanol operating margin over the most recent 30 days. We run the Bayesian MCMC algorithm on the constructed ethanol stock price index and the SPNY index for 50,000 iterations with the first 40,000 draws discarded as burn-in. The last 10,000 iterations are used to estimate model parameters where the means and standard deviations of the posterior samples are calculated as parameter estimates and standard errors, respectively. Table 2 provides the estimation results for the two indices and Figures 3 and 4 present the estimated volatility processes.

The parameter estimates of the SVCMJ model for the ethanol stock index indicate (i) a strong mean-reverting effect in the stochastic volatility process with the speed, $\kappa = 2.41$, and the long-run mean return $\mu * 250 = 0.03 * 250 = 7.50\%$; (ii) a negative correlation between return and instantaneous volatility, $\rho = -0.15$; and (iii) infrequent jumps in returns and volatility. The estimate of the jump intensity parameter $\lambda = 0.0019$ suggests on average $0.0019 * 250 = 0.48$ jumps per year. With only three years of data available, the jump components in returns and volatility are difficult to capture, as indicated by the relatively large standard errors associated with the jump-related parameters, including μ_y , ρ_J , and σ_y .

The dynamic relationships among the volatilities of ethanol and S&P 500 indices as well as uncertainty are presented in Figures 3 and 4. There is a notable structural change in the biofuel price index over the sample period. Before July 2008, ethanol price volatility largely followed the pattern of profit uncertainty. However, the volatility patterns of the ethanol stock index and S&P 500 energy index are strikingly similar in the more recent period. We formally test for the structural change point in the estimated volatility of the ethanol stock index by employing the test proposed in Bai and Perron (1998) and the traditional CUSUM test, which is first introduced in Ploberger and Kramer (1992).⁹ Both tests identify the structural change point at July 15, 2008.

Figure 3 overlays the volatility of ethanol stock prices and uncertainty of ethanol profitability, where the latter is computed daily over the most recent 30 days. As mentioned above, the empirical pattern of stock price volatility is quite similar to that of uncertainty before the structural change that happened in mid-July 2008. The volatility peaks in late 2005 to mid-2006, which was a time of high uncertainty in ethanol

⁹ Although these structural change tests are mainly developed for detecting endogenous breaks in the mean parameters of trend models, as mentioned, they can also accommodate changes in the variance (Bai and Perron 1998). The CUSUM test is employed for robustness check. Further evidence of application of the tests on volatility process can be found in, e.g., Cuñado, Biscarri and Hidalgo (2004).

profitability. This means that while investors anticipated the uncertainty associated with ethanol returns, the risks are fully reflected in the variation of ethanol stock prices. This relationship is further confirmed by the OLS regression of estimated ethanol volatility on uncertainty. The results show a positive (0.63) coefficient of uncertainty on stock volatility, which is statistically significant at the 1% level. Approximately 23% of the volatility variation can be explained by changes in uncertainty.

Figure 4 plots the estimated volatility processes of the ethanol stock index and S&P 500 energy index. Before July 2008, ethanol stocks were more volatile than the general energy stocks, probably due to uncertainty associated with the new technology and/or business model. After July 2008, the evolution of ethanol volatility tracks with that of the S&P 500, which is consistent with the timing of the oil price shock in mid-2008 and the corresponding binding ethanol blending mandate. As the crude oil price reached \$140 in June 2008, there was an expectation that more ethanol facilities would come online. When crude oil prices began to fall, it was clear that additional facilities would not have to be built. In fact it became clear that the government mandate on ethanol consumption would be binding (Babcock 2008). With cheap crude oil, there was low demand for ethanol. The gasoline producers would be forced to buy ethanol even if it was sold at a loss. They offered ethanol producers just enough to stay in business and meet the mandate. Profitability in ethanol was close to zero, and the stock prices reflected this.

5. Conclusion

Employing a stochastic volatility model with correlated jumps in both returns and volatility, we examine the empirical links among volatility of ethanol stock prices, uncertainty associated with profitability of ethanol production and stock price variation in

the traditional energy sector. An ethanol stock price index is constructed to measure the price pattern of publicly traded ethanol stocks over the period June 2005 to July 2009.

With increasing scale of adoption and production of ethanol, a strong and significant correlation is found between ethanol stock volatility and profit uncertainty before July 2008. This supports recent findings in the literature on the relationship between uncertainty and price variation during the evolution of an innovative technology. The volatility process of biofuel stock prices is found to have had a structural change in July 2008, which may have been induced by the interactions between agricultural and energy markets. Biofuel stock price volatility tracked closely with that of the traditional energy sector after that period.

References

- Ait-Sahalia, Y., & Kimmel, R. 2007. Maximum likelihood estimation of stochastic volatility models. *Journal of Financial Economics* 83 (2, February): 413-452.
- Anderson, T.G., Benzoni, L., & Lund, J. 2002. An empirical investigation of continuous-time equity return models. *Journal of Finance* 57 (3, June): 1239-1284.
- Babcock, B.A. 2008. How low will corn prices go? *Iowa Ag Review* 14 (4): 1-3.
- Bai, J., & Perron, P. 1998. Estimating and testing linear models with multiple structural changes. *Econometrica* 66: 47-78.
- Bates, D. 1996. Jumps and stochastic volatility: Exchange rate processes implicit in deutsche mark options. *Review of Financial Studies* 9 (1, Spring): 69-107.
- Brandt, M., & Santa-Clara, P. 2002. Simulated likelihood estimation of diffusions with an application to exchange rate dynamics in incomplete markets. *Journal of Financial Economics* 63 (2, February): 161-210.
- Chernov, M., Gallant A.R., Ghysels, E., & Tauchen G. 2003. Alternative models of stock price dynamics. *Journal of Econometrics* 116: 225-257.
- Cuñado Eizaguirre, J., Biscarri, J., & Hidalgo, F.. 2004. Structural changes in volatility and stock market development: Evidence of Spain. *Journal of Banking & Finance* 28: 1745-1773.
- DeMarzo, P., Kaniel, R., & Kremer, I. 2007. Technological innovation and real investment booms and busts. *Journal of Financial Economics* 85 (3): 735-754.
- Duffie, D., Pan, J., & Singleton K. 2000. Transform analysis and asset pricing for affine jump-diffusions. *Econometrica* 68 (6, November): 1343-1376.
- Eraker, B., Johannes, M., & Polson, N. 2003. The impact of jumps in volatility and returns. *Journal of Finance* 58 (3, June): 1269-1300.

- Gelman, A., Carlin, J., Stern, H., & Rubin, D. 2007. *Bayesian Data Analysis*. Boca Raton, FL: Chapman & Hall/CRC.
- Hall, R. 2001. The stock market and capital accumulation. *American Economic Review* 91 (5): 1185-1202.
- Henriques, I., & Sadorsky, P. 2008. Oil price and the stock price of alternative energy companies. *Energy Economics* 30: 998-1010.
- Heston, S. 1993. A closed-form solution for options with stochastic volatility with applications to bond and currency options. *Review of Financial Studies* 6: 327-343.
- Hobijn, B., & Jovanovic, B. 2001. The information technology revolution and the stock market: Evidence. *American Economic Review* 91 (5): 1203-1220.
- Jacquier, E., Polson, N., & Rossi, P. 1994. Bayesian analysis of stochastic volatility models (with discussion). *Journal of Business and Economic Statistics* 12: 371-389.
- Johnson, T. 2007. Optimal learning and new technology bubbles. *Journal of Monetary Economics* 54: 2486-2511.
- Laitner, J., & Stolyarov, D. 2003. Technological change and the stock market. *American Economic Review* 93 (4): 1240-1267.
- Li, H., Wells, M., & Yu, C. 2008. A Bayesian analysis of return dynamics with stochastic volatility and Levy jumps. *Review of Financial Studies* 21 (5): 2345-2378.
- Nelson, D.B. 1991. Conditional heteroskedasticity in asset return: A new approach. *Econometrica* 59 (2, March): 347-370.
- Nicholas, T. 2008. Does innovation cause stock market runups? Evidence from the Great Crash. *American Economic Review* 98 (4): 1370-1396.
- Pan, J. 2002. The jump-risk premia implicit in options: Evidence from an integrated time-series study. *Journal of Financial Economics* 63 (1, January): 3-50.

- Pastor, L., & Veronesi, P. 2003. Stock valuation and learning about profitability. *Journal of Finance* 58: 1749-1789.
- . 2006. Was there a NASDAQ bubble in the late 1990s? *Journal of Financial Economics* 81: 61-100.
- . 2009. Technological revolution and stock prices. *American Economic Review*, 99 (4): 1451-1483.
- Ploberger, W., & Kramer, W. 1992. The CUSUM test with OLS residuals. *Econometrica* 60: 271-285.
- Renewable Fuels Association (RFA). 2009. Historic U.S. fuel ethanol production. Available at: <http://www.ethanolrfa.org/industry/statistics/>. Last access 9/16/2009.
- Wall Street Journal (WSJ). 2008. The death of ethanol: One thing Wall Street saw coming. November 3.

Table 1. Companies included in the ethanol stock price index.

| Name | Symbol | Market Capitalization (as of 15 Nov 2009, in million U.S. dollars) | Weight | Sample Period |
|---|----------------------------|--|--------|------------------------|
| Archer Daniels Midland | NYSE: ADM | 18290 | 1 | 30 Jun 2005–9 Jul 2009 |
| Cosan Limited | NYSE: CZZ | 2300 | 0.33 | 16 Aug 2007–9 Jul 2009 |
| The Andersons, Inc. | NASDAQ: ANDE | 622.20 | 0.33 | 30 Jun 2005–9 Jul 2009 |
| Green Plains Renewable Energy, Inc. | NASDAQ: GPRE | 183.92 | 0.1 | 15 Mar 2006–9 Jul 2009 |
| MGP Ingredients, Inc. | NASDAQ: MGPI | 66.73 | 0.1 | 30 Jun 2005–9 Jul 2009 |
| Pacific Ethanol, Inc. | NASDAQ: PEIX | 28.30 | 0.33 | 30 Jun 2005–9 Jul 2009 |
| BioFuel Energy Corp. | NASDAQ: BIOF | 23.09 | 0.25 | 14 Jun 2007–9 Jul 2009 |
| Aventine Renewable Energy Holdings, Inc. | OTC: AVRNQ | 7.95 | 0.33 | 29 Jun 2006–9 Jul 2009 |
| Global Energy Holdings Group, Inc. (former Xethanol Corp.) | AMEX: GNH (former XNL) | 4.94 | 0.1 | 30 Jun 2005–9 Jul 2009 |
| Cono Italiano, Inc. (former Tiger Renewable Energy) | OTC: CNOZ (former TGRW) | 1.45 | 0.1 | 11 Dec 2006–9 Jul 2009 |
| VeraSun Energy | NYSE: VSE (delisted) | N/A | 0.33 | 14 Jun 2006–9 Jul 2009 |

Table 2. Estimation results of biofuel stock price index and S&P 500 energy sector index.

| | Ethanol Stock Index | | S&P 500 Energy Index | |
|------------|---------------------|--------------|----------------------|------------|
| | Mean | Stand. Error | Mean | Std. Error |
| μ | 0.03 | 0.20 | 0.28 | 0.19 |
| μ_y | 0.66 | 1.96 | -5.40 | 1.65 |
| μ_v | 1.07 | 0.25 | 1.10 | 1.10 |
| ρ_J | 0.33 | 0.86 | 0.26 | 0.26 |
| σ_y | 2.30 | 0.69 | 2.04 | 2.04 |
| λ | 0.0019 | 0.0014 | 0.0019 | 0.0014 |
| θ | 1.43 | 0.43 | 1.37 | 0.44 |
| κ | 2.41 | 0.69 | 2.24 | 0.71 |
| σ_v | 2.49 | 0.14 | 2.37 | 0.12 |
| ρ | -0.15 | 0.10 | -0.07 | 0.10 |

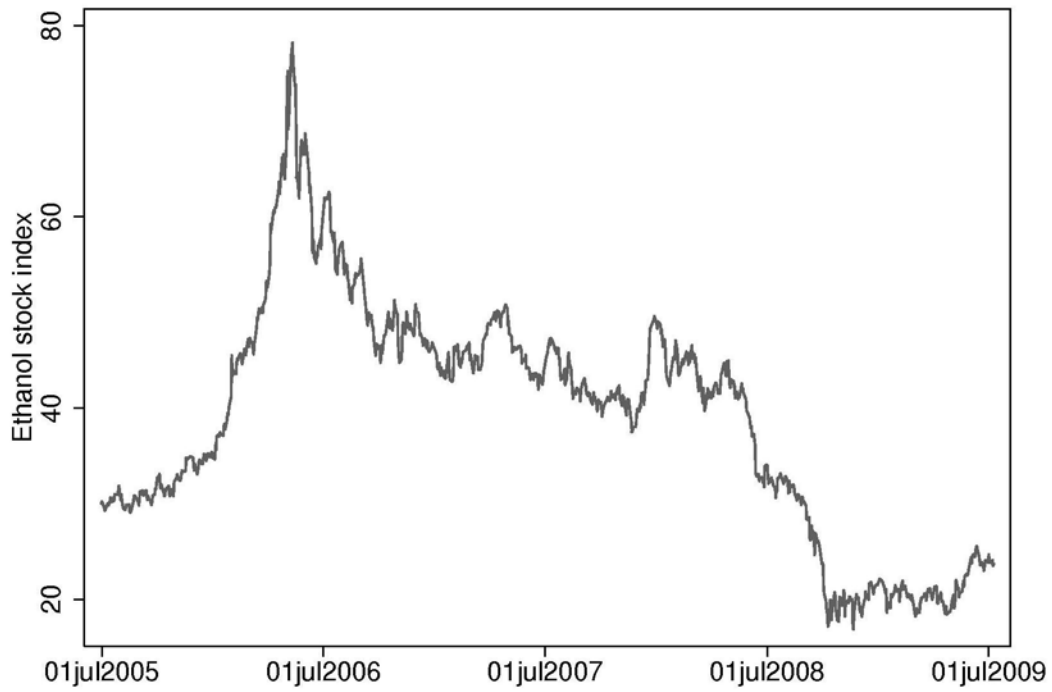


Figure 1. Constructed ethanol stock price index, 30 June 2005–9 July 2009.

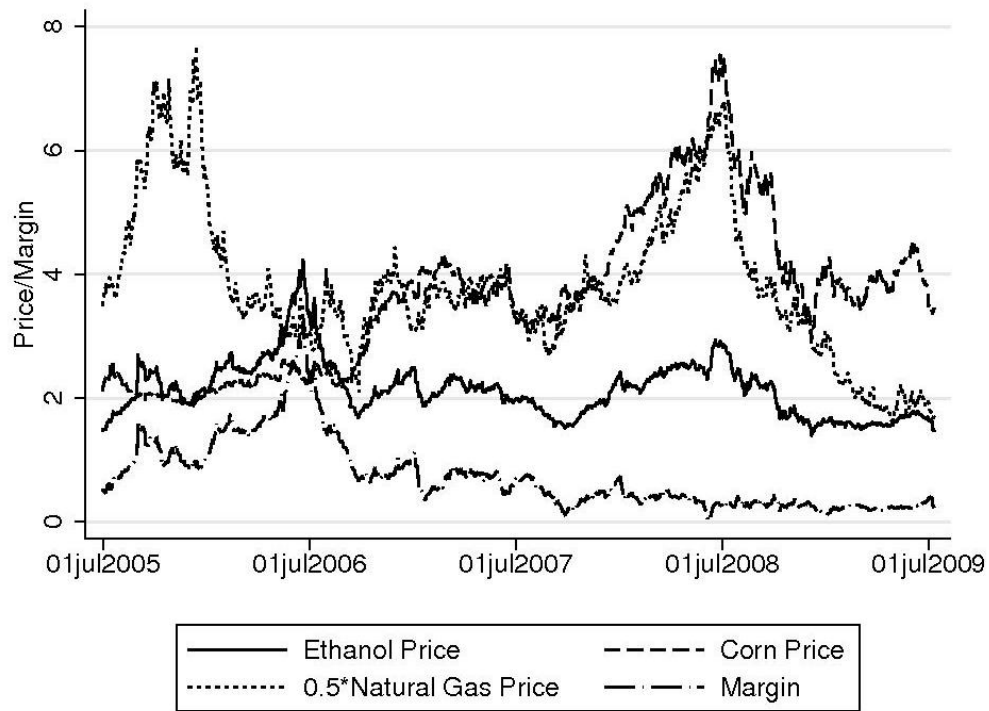


Figure 2. Ethanol, corn, and natural gas prices and ethanol operating margins, 30 June 2005–9 July 2009.

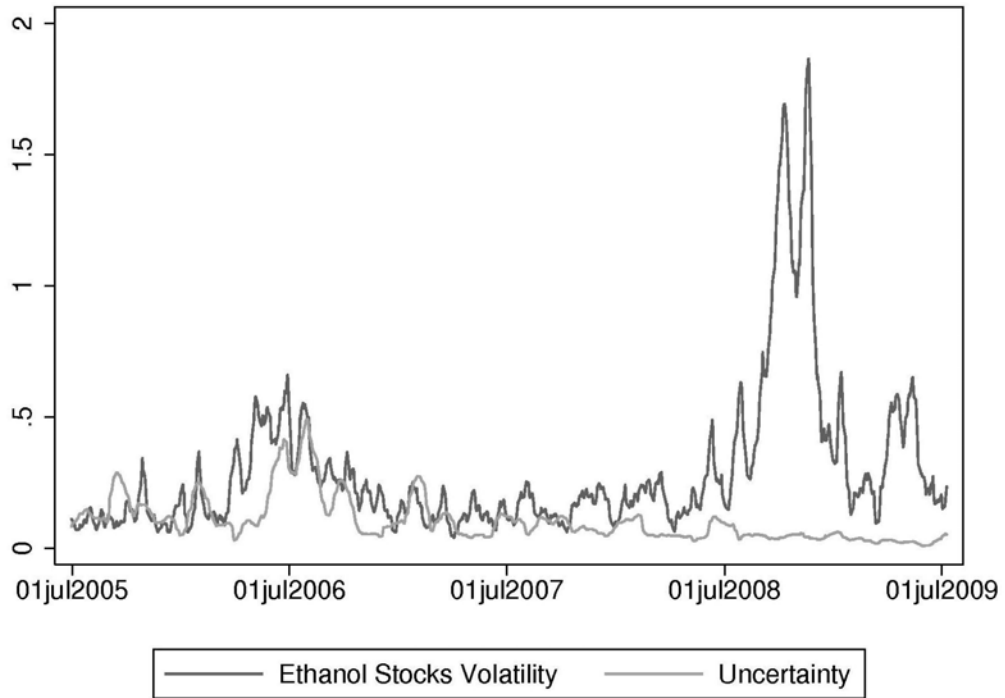


Figure 3. Ethanol stock volatility and profit uncertainty, 30 June 2005–9 July 2009.

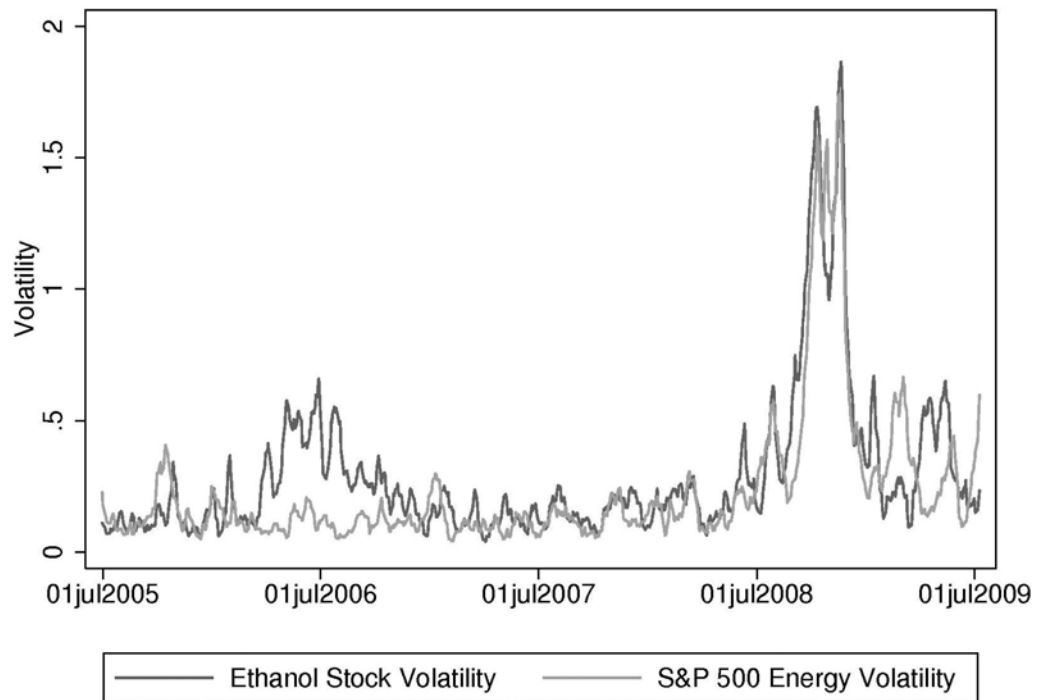


Figure 4. Volatilities of ethanol stock index and S&P 500 energy sector index, 30 June 2005–9 July 2009.

Appendix A: The Posterior Simulator

In the following, we describe the Gibbs sampling algorithm employed for simulating the parameters of interest from their derived posterior distributions. Here, we let $\Theta_{\{-x\}}$

denote all parameters in the set Θ except x , the one being simulated.

Step 1. $\mu \mid \mathbf{Y}, \mathbf{V}, \mathbf{N}, \xi^y, \xi^v, \Theta_{\{-\mu\}} \sim N(S/W, 1/W)$

$$\text{where } W = \frac{\Delta}{1-\rho^2} \sum_{t=1}^T \left(\frac{1}{V_t} \right) + \frac{1}{M^2}, \quad S = \frac{1}{1-\rho^2} \sum_{t=1}^T \frac{1}{V_t} \left(C_t - \rho \frac{D_t}{\sigma_v} \right) + \frac{m}{M^2},$$

$$C_t = Y_{t+1} - Y_t - N_t \xi_t^y, \text{ and } D_t = V_{t+1} - V_t - \kappa(\theta - v_t)\Delta - N_t \xi_t^v. \quad m \text{ and } M \text{ are the}$$

hyperparameters for the prior distribution of the corresponding parameter (the same hereafter).

Step 2: $\mu_y \mid \mathbf{Y}, \mathbf{V}, \mathbf{N}, \xi^y, \xi^v, \Theta_{\{-\mu_y\}} \sim N(S/W, 1/W)$

$$\text{where } W = \frac{T}{\sigma_y^2} + \frac{1}{M^2}, \quad S = \frac{\sum_{t=1}^T (\xi_t^y - \rho_J \xi_t^v)}{\sigma_y^2} + \frac{m}{M^2}.$$

Step 3: $\mu_v \mid \mathbf{Y}, \mathbf{V}, \mathbf{N}, \xi^y, \xi^v, \Theta_{\{-\mu_v\}} \sim IG\left(T + m, 1 / \left(\sum_{t=1}^T \xi_t^v + 1/M\right)\right).$

Step 4: $\rho_J \mid \mathbf{Y}, \mathbf{V}, \mathbf{N}, \xi^y, \xi^v, \Theta_{\{-\rho_J\}} \sim N(S/W, 1/W)$

$$\text{where } W = \frac{\sum_{t=1}^T (\xi_t^v)^2}{\sigma_y^2} + \frac{1}{M^2}, \quad S = \frac{\sum_{t=1}^T \xi_t^v C_t}{\sigma_y^2} + \frac{m}{M^2}, \quad C_t = \xi_t^y - \mu_y.$$

Step 5: $\sigma_y^2 \mid \mathbf{Y}, \mathbf{V}, \mathbf{N}, \xi^y, \xi^v, \Theta_{\{-\sigma_y^2\}} \sim IG\left(\frac{T}{2} + m, \frac{1}{1/2 \sum_{t=1}^T (\xi_t^y - \mu_y - \rho_J \xi_t^v)^2 + 1/M}\right)$

Step 6: $\lambda \mid \mathbf{Y}, \mathbf{V}, \mathbf{N}, \xi^y, \xi^v, \Theta_{\{-\lambda\}} \sim \text{Beta}\left(\sum_{t=1}^T N_t + m, T - \sum_{t=1}^T N_t + M\right)$

Step 7: $\theta | \mathbf{Y}, \mathbf{V}, \mathbf{N}, \xi^y, \xi^v, \Theta_{\{-\theta\}} \sim TN_{(0,\infty)}(S/W, 1/W)$

$$\text{where } W = \frac{\kappa^2 \Delta}{\sigma_v^2 (1-\rho^2)} \sum_{t=1}^T \frac{1}{V_t} + \frac{1}{M^2}, \quad S = \frac{\kappa}{(1-\rho^2)\sigma_v} \sum_{t=1}^T \left(\frac{D_t / \sigma_v - \rho C_t}{V_t} \right) + \frac{m}{M^2},$$

$$C_t = Y_{t+1} - Y_t - \mu\Delta - N_t \xi_t^y, \text{ and } D_t = V_{t+1} + (\kappa\Delta - 1)V_t - N_t \xi_t^v.$$

Step 8: $\kappa | \mathbf{Y}, \mathbf{V}, \mathbf{N}, \xi^y, \xi^v, \Theta_{\{-\kappa\}} \sim TN_{(0,\infty)}(S/W, 1/W)$

$$\text{where } W = \frac{\Delta}{\sigma_v^2 (1-\rho^2)} \sum_{t=1}^T \frac{(\theta - V_t)^2}{V_t} + \frac{1}{M^2},$$

$$S = \frac{1}{(1-\rho^2)\sigma_v} \sum_{t=1}^T \left(\frac{(\theta - V_t)(D_t / \sigma_v - \rho C_t)}{V_t} \right) + \frac{m}{M^2}, \quad C_t = Y_{t+1} - Y_t - \mu\Delta - N_t \xi_t^y, \text{ and}$$

$$D_t = V_{t+1} - V_t - N_t \xi_t^v.$$

$$\text{Step 9: } \omega_v | \mathbf{Y}, \mathbf{V}, \mathbf{N}, \xi^y, \xi^v, \Theta_{\{-\rho, \sigma_v\}} \sim IG \left(\frac{T}{2} + m, \frac{1}{1/2 \sum_{t=1}^T D_t^2 + 1/M - S^2/2W} \right) \text{ and}$$

$$\phi_v | \omega_v \sim N(S/W, \omega_v/W)$$

$$\text{where } W = \sum_{t=1}^T C_t^2 + 2, \quad S = \sum_{t=1}^T C_t D_t, \quad C_t = (Y_{t+1} - Y_t - \mu\Delta - N_t \xi_t^y) / \sqrt{V_t \Delta}, \text{ and}$$

$$D_t = (V_{t+1} - V_t - \kappa(\theta - V_t)\Delta - N_t \xi_t^v) / \sqrt{V_t \Delta}.$$

Then (ϕ_v, w_v) are inverted back to get (ρ, σ_v) after each posterior draw of (ϕ_v, w_v) .

$$\text{Step 10: } N_t | \mathbf{Y}, \mathbf{V}, \xi^y, \xi^v, \Theta \sim \text{Bernoulli} \left(\frac{\alpha_1}{\alpha_1 + \alpha_2} \right)$$

where $\alpha_1 = \exp\left\{-\frac{1}{2(1-\rho^2)}[A_1^2 - 2\rho A_1 B_1 + B_1^2]\right\} \lambda$,

$\alpha_2 = \exp\left\{-\frac{1}{2(1-\rho^2)}[A_2^2 - 2\rho A_2 B_2 + B_2^2]\right\} (1-\lambda)$, $A_1 = (Y_{t+1} - Y_t - \mu\Delta - \xi_t^y) / \sqrt{v_t\Delta}$,

$A_2 = (Y_{t+1} - Y_t - \mu\Delta) / \sqrt{V_t\Delta}$, and $B_1 = (V_{t+1} - V_t - \kappa(\theta - V_t)\Delta - \xi_t^v) / (\sigma_v \sqrt{V_t\Delta})$,

$B_2 = (V_{t+1} - V_t - \kappa(\theta - V_t)\Delta) / (\sigma_v \sqrt{V_t\Delta})$.

Step 11: The posterior draw of (ζ_t^y, ζ_t^v) are jointly drawn from the following distribution.

$\xi_t^v | \mathbf{Y}, \mathbf{V}, \mathbf{N}, \Theta \sim TN_{(0,\infty)}(S_2 / W_2, 1 / W_2)$, $\xi_t^y | \xi_t^v, \mathbf{Y}, \mathbf{V}, \mathbf{N}, \Theta \sim TN_{(0,\infty)}(S_1 / W_1, 1 / W_1)$.

where $W_2 = \frac{N_t^2}{(1-\rho^2)\sigma_v^2 V_t\Delta} + \frac{\rho_J^2}{\sigma_y^2} - \frac{B^2}{W_1}$,

$S_2 = \frac{N_t}{(1-\rho^2)\sigma_v V_t\Delta} (-\rho C_t + \frac{D_t}{\rho_v}) - \frac{\mu_y \rho_J}{\sigma_y^2} - \frac{1}{\mu_v} + \frac{AB}{W_1}$, $W_1 = \frac{N_t^2}{(1-\rho^2)V_t\Delta} + \frac{1}{\sigma_y^2}$, $S_1 = A + B\xi_t^v$,

$A = \frac{N_t}{(1-\rho^2)V_t\Delta} (C_t - \frac{\rho D_t}{\sigma_v}) + \frac{\mu_y}{\sigma_y^2}$, $B = \frac{\rho N_t^2}{(1-\rho^2)\sigma_v V_t\Delta} + \frac{\rho_J}{\sigma_y^2}$, $C_t = Y_{t+1} - Y_t - \mu\Delta$, and

$D_t = V_{t+1} - V_t - \kappa(\theta - V_t)\Delta$.

Step 12: The posterior distribution of v_{t+1} is time-varying.

for $1 < t < T$,

$p(V_t | \mathbf{Y}, \mathbf{N}, \xi_t^y, \xi_t^v, \Theta) \propto \exp\left\{-\frac{[-2\rho\zeta_t^y \zeta_t^v + (\zeta_t^y)^2]}{2(1-\rho^2)}\right\} \times \frac{1}{V_t} \times \exp\left\{-\frac{[\zeta_{t+1}^y - 2\rho\zeta_{t+1}^y \zeta_{t+1}^v + (\zeta_{t+1}^v)^2]}{2(1-\rho^2)}\right\}$

where $\zeta_t^y = (Y_{t+1} - Y_t - \mu\Delta - N_t \xi_t^y) / \sqrt{V_{t-1}\Delta}$,

$\zeta_t^v = (V_{t+1} - V_t - \kappa(\theta - V_t)\Delta - N_t \xi_t^v) / (\sigma_v \sqrt{v_{t-1}\Delta})$.

For $t = 1$,

$$p(V_1 | \mathbf{Y}, \mathbf{N}, \xi^y, \xi^v, \Theta) \propto \frac{1}{V_1} \times \exp \left\{ -\frac{[\zeta_2^y - 2\rho\zeta_2^y\zeta_2^v + (\zeta_2^v)^2]}{2(1-\rho^2)} \right\}.$$

For $t = T + 1$,

$$p(V_{T+1} | \cdot) \propto \exp \left\{ -\frac{[-2\rho\zeta_{T+1}^y\zeta_{T+1}^v + (\zeta_{T+1}^v)^2]}{2(1-\rho^2)} \right\}.$$

Given the complicated distribution forms, it is difficult to sample from this posterior distribution of V_t . To update the latent volatility variables, we employ the random walk Metropolis-Hasting algorithm (Gelman et al. 2007).

Appendix B: Simulation study

The MCMC algorithm described in Section 2.2 is applied on a simulated data set to measure its accuracy. The program, written in Matlab, has a posterior sample size of 50,000 for each run with the first 40,000 discarded as burn-in period. The sample mean and standard error of the last 10,000 posterior draws as well as the true parameter values used for simulation are reported in Table B-1. Figure B-1 presents the generated (true) and estimated volatility processes, while the generated and estimated jumps in return and volatility are shown in Figure B-2.

The results in Table B-1 indicate that the algorithm provides relatively accurate estimates for most of the model parameters except the drift parameter μ . As Ait-Sahalia and Kimmel (2007) point out, the estimation of drift term is difficult, requiring a long period of samples to improve the quality of the estimate. As the volatility estimation is the major concern in this study, Figures B-1 and B-2 show that our algorithm is capable of capturing major dynamics of the volatility path and jumps in both returns and volatility processes.

Table B-1. Estimation results on simulated data set.

| | μ | μ_y | μ_v | ρ_J | σ_y | λ | θ | κ | σ_v | ρ |
|-----------|-------|---------|---------|----------|------------|-----------|----------|----------|------------|--------|
| True | 0.05 | 3.00 | 1.00 | -0.40 | 3.50 | 0.015 | 0.80 | 1.20 | 2.00 | -0.40 |
| Mean | 0.014 | 2.93 | 0.92 | -0.54 | 2.39 | 0.023 | 0.84 | 1.32 | 1.68 | -0.39 |
| Std. err. | 0.53 | 0.75 | 0.14 | 0.70 | 0.35 | 0.0047 | 0.52 | 0.50 | 0.14 | 0.14 |

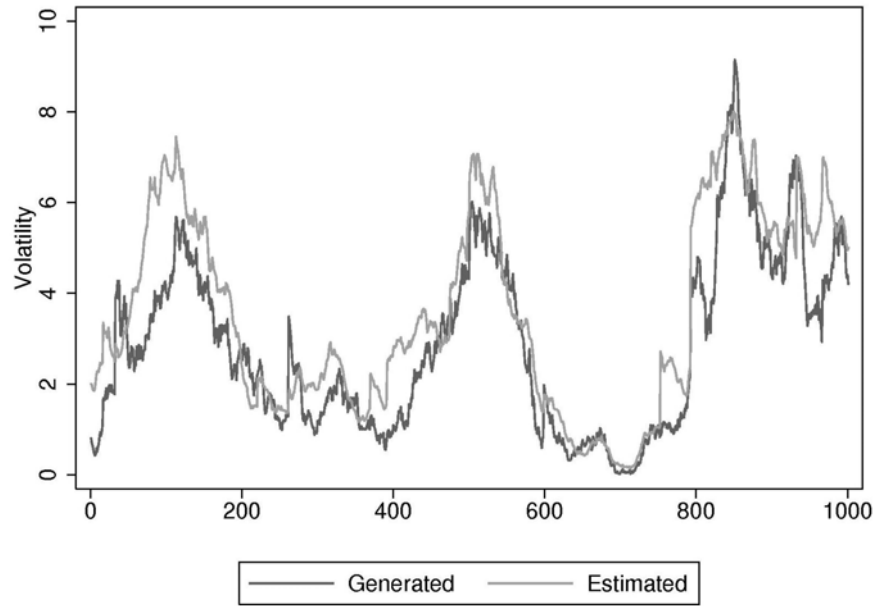


Figure B-1. Volatility estimation results of simulated data set.

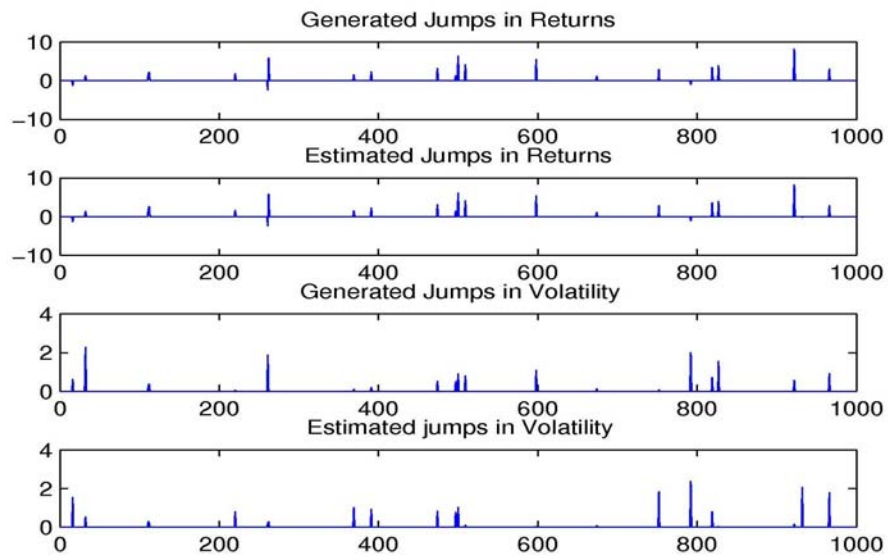


Figure B-2. Jumps estimation results of simulated data set.